Structural Chemistry, Vol. 16, No. 3, June 2005 (© 2005)
DOI: 10.1007/s11224-005-4445-x

Theoretical Investigation of Normal to Strong Hydrogen Bonds

Chaeho Pak,[1] Han Myoung Lee,[1] Jong Chan Kim,[1] Dongwook Kim,[1] and Kwang S. Kim[1,2]

Received May 13, 2004; revised August 11, 2004; accepted August 12, 2004

We review our theoretical work done on a variety of different chemical systems, which show different H-bonding characteristics. The systems include water clusters, its interactions with polar molecules and π-systems, organic nanotubes, enzymes, and ionophores/receptors. Special features of normal, short, short strong, and π-type H-bonding interactions in these systems are discussed in terms of structures, interaction energies, and spectra.

KEY WORDS: Hydrogen bond; *ab initio* calculations; water; ionophore; enzyme.

INTRODUCTION

Nature is composed of a variety of different chemical bonds. Life exists merely because there are atoms and molecules, and intra and intermolecular forces governing them [1, 2]. One of the most vital forces, H-bond, plays important roles both in chemistry and biology. For instance, the most abundant and essential substance on our planet, water, and the most important substance in biosystems, proteins and DNA are held basically by networks of H-bonds. The H-bond energy ranges from 1 to 30 kcal/mol. Since H-bonds can be easily formed and broken depending on the given environment, they are considered to have "on or off" functions in biology [1].

Although H-bond is one of the very important intermolecular forces, it is still poorly understood partially due to their weak long-range interactions and their shallow, anisotropic, and anharmonic nature of potential energy surface. However, recent progress both in theoretical and experimental methods has shown many new interesting facts about the H-bonding. Then, these H-bond interactions have been applied to the biological and material chemistry [3–8]. H-bonds have often been used for self-assembling macromolecular architecture such as capsules, nanotubes, wires, etc. [4]. The charge transfer (CT) through the H-bonded networks of a wire form has been chemically and biochemically explored [5]. The charged and ionic H-bond interactions have been applied to the recognition of ions by receptors/ionophores [6]. Many biological systems such as proteins, membranes, RNA, and DNA show functions related to multiply H-bonded frames [7].

Among many different methods for studying H-bonds, due to much progress in development of highly efficient computational algorithm, computer hardware, and new theoretical models, *ab initio* molecular orbital calculation has become probably the method of choice for studying H-bonds. This is in part because theoretical investigations make it easy to explore potential energy surface in a variety of different conformations and deduce different electronic energy components such as electrostatic, inductive, dispersive, charge transfer and repulsive, as well as their influences on the structures, spectra, and interaction energies. These energy components have different physical origin, magnitude, and directionality. Electrostatic forces result from interactions between permanent electric multipole moments of complex partners; induction forces result from interactions of permanent electric multipole moment of one monomer with electric multipole moment induced in the other monomer; dispersion forces result from mutual polarization of electron densities of two interacting monomers; charge transfer refers to electron transfer between occupied orbitals and vacant orbitals between different atoms; repulsive forces result from the Pauli exclusion principle, which prevents the electrons of one monomer from penetrating into the occupied space of the other monomer. This exchange repulsion

[1]National Creative Research Initiative Center for Superfunctional Materials, Department of Chemistry, Division of Molecular and Life Sciences, Pohang University of Science and Technology, San 31, Hyojadong, Namgu, Pohang 790-784, Korea.
[2]To whom all correspondence should be addressed; e-mail: kim@postech.ac.kr.

increases with increasing overlap and is always destabilizing. Depending on the nature of H-bonds, it can have different proportions of these energy components. For example, in the case of strong H-bond [F^-—H—F], the charge transfer accounts for more than 40% of the interaction energy [1].

Even though it is tempting to cover all the aspects of H-bonds, due to vast amount of materials, it is impractical for this short review. Instead, interested readers can find many books [1, 2], and reviews [8, 9] concerning this topic. In this review, we will summarize our theoretical work done on many different chemical systems (gas phase water clusters, organic nanotubes, enzymes, and receptors), which exhibit wide variety of different H-bonding characteristics such as normal, short, short strong, and π-type H-bonds. Some of the pertinent issues which will be addressed in the course of this review are the following: (i) the changes in the interaction and binding energies due to the cluster size on the example of water, (ii) the cooperativity effect on molecular properties, (iii) the binding energies for charged H-bonds in enzymes and bio-receptors, and (iv) normal versus strong hydrogen bonds.

H-BOND IN SMALL POLAR AND π-SYSTEMS

The H-bond interactions can be noted as X–$H^{\delta+}\cdots^{\delta-}$Y, where X is a polar proton donor and Y a proton acceptor or an electronegative ion with lone pairs of electrons. Depending on the nature of X and Y, the strength of H-bonds varies. For example, when X and Y are a good proton donor and a good proton acceptor, respectively, they form a very strong H-bond. Figure 1 shows interaction of water molecule with a variety of different small polar (H_2O, H_2S, NH_3, PH_3, HF, HCl,

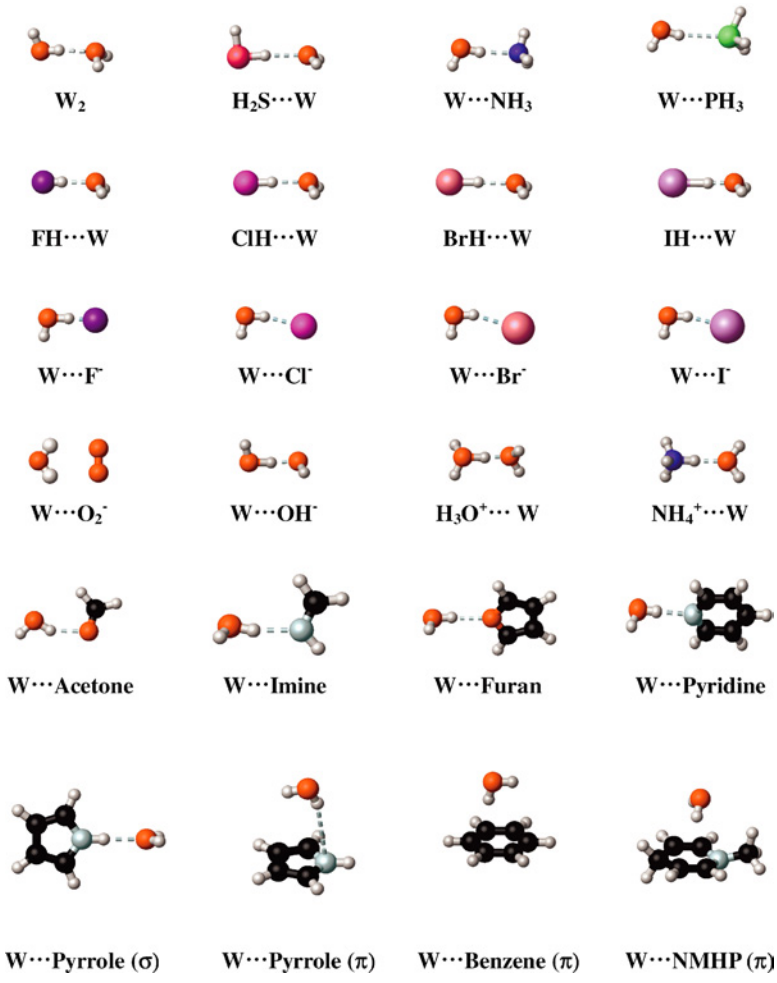

Fig. 1. H-bonded dimers of neutral, charged, and σ versus π H-bonds. W and NMHP denotes for H_2O and *N*-methyl-4-hydropyridine, respectively.

HBr, HI [10]) cationic (H_3O^+, NH_4^+ [11]), anionic (F^-, Cl^-, Br^-, I^-, OH^- [12]), and σ versus π-systems (acetone, imine, furan, pyridine, pyrrole, and *N*-methyl-4-hydropyridine (NMHP) [9, 13]). There are also many similar studies [14]. Table I shows their interaction energies [zero-point-energy (ZPE)-corrected energies: ΔE_0] using the density functional theory employing Becke's three parameters with Lee–Yang–Parr functionals (B3LYP)/6–311++G** and the Moller–Plesset second-order perturbation theory (MP2)/aug-cc-*p*VDZ+(2*s*2*p*/2*s*) [16]. The interaction energies are reported as the median value of the basis set superposition error (BSSE)-corrected and BSSE-uncorrected values, which can be considered as the lower and upper limits [9]. Although the BSSE-corrected values are more rigorous in theoretical viewpoint, the energy obtained from incomplete basis sets is underestimated due to the lack of insufficient electron correlation energy, which in most cases tends to be empirically compensated partially by BSSE. In particular, it should be noted that the BSSE-uncorrected H-bond distance is somewhat too short, so that the full BSSE correction underestimates the binding energy due to the overestimated repulsion at the distance (toward the hard wall region) shorter than the optimal H-bond distance.

Table I. MP2/aug-cc-pVDZ + (2s2p/2s) [B3LYP/6-311++G**] Zero-Point-Energy Corrected Interaction Energies (kcal/mol) of Various Molecules with a Water Molecule

	$-\Delta E_0$
H_2O	2.56 ± 0.42 [3.13 ± 0.41]
H_2S	1.34 ± 0.36 [1.39 ± 0.28]
PH_3	1.10 ± 0.36 [0.95 ± 0.19]
NH_3	4.08 ± 0.57 [4.60 ± 0.38]
HF	6.26 ± 0.59 [7.37 ± 0.56]
HCl	4.20 ± 0.52 [4.45 ± 0.44]
HBr	3.51 ± 0.60 [3.55 ± 0.37]
HI	2.66 ± 0.42 [2.03 ± 0.26]
F^-	25.24 ± 0.75 [27.40 ± 0.55]
Cl^-	13.05 ± 0.48 [13.51 ± 0.15]
Br^-	11.55 ± 0.70 [12.03 ± 0.09]
I^-	9.43 ± 0.63 [9.43 ± 0.08]
O_2^-	18.56 ± 0.71 [20.21 ± 0.44]
OH^-	24.52 ± 0.98 [26.65 ± 0.43]
H_3O^+	33.52 ± 1.15 [35.83 ± 0.72]
NH_4^+	18.30 ± 0.69 [20.14 ± 0.42]
Acetone	3.60 ± 0.52 [2.84 ± 0.14]
Imine	4.82 ± 0.59 [4.38 ± 0.20]
Furan	2.55 ± 0.51 [1.74 ± 0.23]
Pyridine	5.82 ± 0.70 [4.86 ± 0.25]
σ_H-Pyrrole	4.74 ± 0.58 [4.04 ± 0.41]
π_H-Pyrrole	4.65 ± 0.92 [2.02 ± 0.26]
π_H-Benzene	2.86 ± 1.13 [1.53 ± 0.22]
π_H-NMHP	5.51 ± 1.14 [1.88 ± 0.49]

Note. ΔE_0 is the median value of BSSE-corrected and -uncorrected binding energies with ZPE correction. The value added/subtracted by a half BSSE is the upper and lower limits which are the BSSE-uncorrected and -corrected binding energies, respectively. Values in brackets were obtained at the B3LYP/6-311++G** level. NMHP denotes *N*-methyl-4-hydropyridine.

Ammonia has strong proton affinity, thus has strong H-bond interactions with the water monomer compared with the interaction in the water dimer (4.08 kcal/mol vs. 2.56 kcal/mol in ΔE_0). In NH_3–H_2O interaction, a polarizable lone-pair electrons in NH_3 makes NH_3 better H-accepting than H_2O. H_2S is a weaker proton acceptor than H_2O, and plays a role of H-donor in H_2O–H_2S interaction. The third elements P and S atoms have relatively weak H-bond interactions due to large atomic radius.

In the hydrogen halide acid–water clusters [10], water plays a role of H-acceptor, while in anion–water clusters [12], water acts as H-donor as shown in Fig. 1. Good acids provide protons more easily than stable anions. Their properties are strongly related to the stabilization of chemicals and dissociated ions by the hydration effect. The anionic systems have strong proton affinity, which gives a strong H-bond interaction. In the case of charged systems [11, 12], the charge highly increases the strength of H-bond interaction due to the strong electrostatic interaction. In the protonated systems, the hydronium cation is a better proton-donor than the ammonium cation [17], so hydronium has stronger H-bond interaction than ammonium. The positively charged systems have stronger H-bond interactions than the negative-charged ones. The positively charged atom can easily interact with the water O atom at a shorter distance, while the negatively charged atom interacts with only a few H atom without full coordination, due to the presence of an excess electron that requires a large vacant space around the anion for stabilization as well as the repulsions between crowded H atoms of water.

Many electronegative atoms have different hybridizations, which can have different effects on H-bond interactions. The different hybridizations appear in double and triple bonds, and in aromatic rings. Some interesting N-containing aromatic rings were theoretically and experimentally investigated for their H-bond interactions with water molecules. Pyridine, which has sp^2-hybridized nitrogen atom and resonance effect, has stronger H-bonding interaction than those of ammonia–water, imine–water, and furan–water systems. This is because the lone-pair electrons of pyridine are less-stabilized and less-delocalized ("localization effect") in the highest-occupied molecular orbital (HOMO), while the lone-pair electrons of furan are delocalized and stabilized at the HOMO (π-electrons occupy carbon atom's HOMO). Pyridine is a good proton-acceptor and therefore plays actively in the H-bond interaction. Pyrrole shows strong

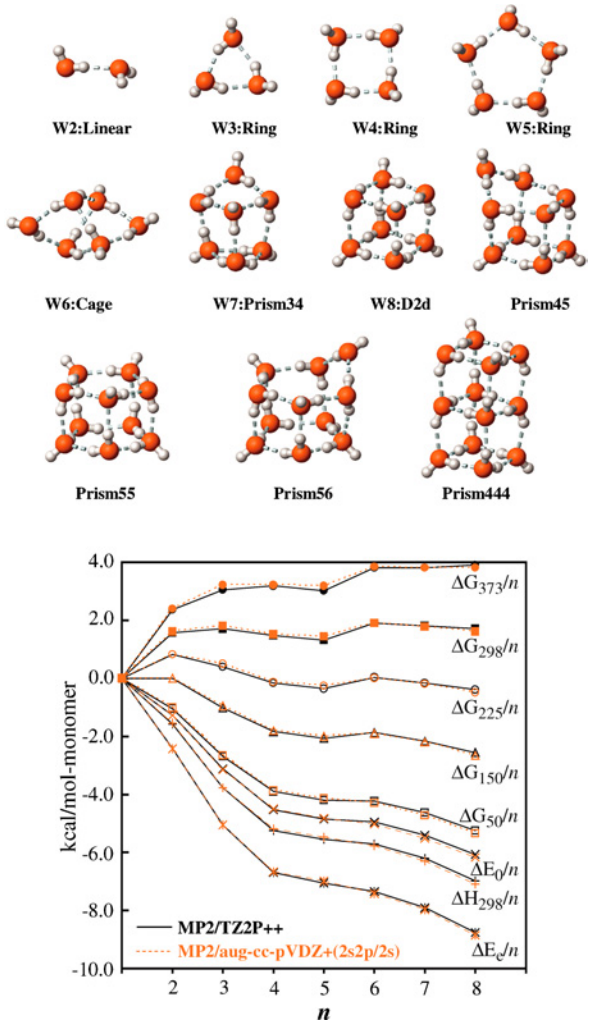

Fig. 2. The lowest-energy neutral water cluster structures (W_{2-12} at 0 K) and the thermodynamic energy changes (W_{2-8}) depending on temperature.

σ H-bond interactions with water due to resonance effect and acidity, and also weak π-H bond interactions with water molecules. In the latter case, the lone-pair electrons are delocalized around the aromatic ring or resonating ring by the resonance effect. The carbon π-electrons are compatible with lone-pair electrons of water molecules. The pictures of their π-type interactions with water show the π-H interaction.

H-BOND IN NEUTRAL WATER CLUSTERS

A water molecule has two lone pairs of electrons and two positively charged hydrogen atoms. Therefore, a water molecule favors four H-bond interactions. Neutral water structures are determined mainly by the H-bond interactions and strains between water molecules. Structures, energetics, and electronic and spectroscopic properties of small water clusters have been well investigated [18–20]. In cluster-scale, water molecules can be classified as "d," "a," "da," "aa," "daa," "dd," "dda" and "ddaa"-types, where "d" and "a" indicate H-donor and H-acceptor, respectively.

The lowest-energy water clusters from water dimer to dodecamer and their interaction energies are presented in Fig. 2 and Table II. As the H-bond interaction is weak and flexible, their conformation and energetics are temperature-dependent due to the entropy effect. Figure 2 shows the interaction energies of water dimer to octamer as a function of temperature. The water tetramer, pentamer, and octamer are relatively stable with respect to the water dimer, hexamer and heptamer. The dimer to pentamer have global minimum energy structures of cyclic ring conformation. However, as in Fig. 3, the hexamer has five iso-energetic conformations. The high level calculations show that the cage structure has the lowest energy, followed by book, prism, cyclic, and bag structures [19]. The calculated interaction energies are summarized in Table III. Indeed, the cage structure which is most stable conformer of neutral water hexamer near 0 K, was experimentally observed [21]. The nearly isoenergetic conformer, book structure was recently observed [22]. In addition, the slightly higher energy conformer of cyclic structure was observed in Ar matrix [23].

As the cluster size increases from the water dimer to hexamer, the average O—O distance of H-bonded water cluster decreases with the increased H-bond strength. The O—H stretch modes of the non-cyclic water hexamer and heptamer do not show further red-shifts with respect to those of the water hexamer, because their O—O distances are almost the same as that of the cyclic hexamer. These O—O distances are useful for comparing their strengths of H-bond interactions, and are also related to the red-shifts of the stretch modes. The structures, energetics, and spectra of the lowest energy water clusters from the nonamer to dodecamer can be formed in our previous work [18].

Generally, single H-donor water molecules ("da" or "daa" waters) have strong H-bond interactions in neutral water clusters. This aspect appears in IR spectra for O—H stretching frequencies as strong red-shifts. Water trimer to pentamers with cyclic mono-ring structures exhibit strong H-bond interactions. The red-shifts of O—H stretch frequencies monotonically increase up to the hexamer ring structure owing to the increase of the strength of H-bond interaction by the decrease of bond angle strains (Fig. 4 and Table IV). However, this H-bond strength is saturated at the hexamer, and so the heptamer and

Table II. Interaction Energies (kcal/mol) of Neutral Water Clusters, $(H_2O)_{n=2-12}$

			MP2/TZ2P++				MP2/aug-cc-pVDZ + (2*s*2*p*/2*s*)			
n	Structure	#HB	$-\Delta E_e \pm$ BSSE/2	$-\Delta E_0$	$-\Delta H_{298}$	$-\Delta G_{50}$	$-\Delta E_e \pm$ BSSE/2	$-\Delta E_0$	$-\Delta H_{298}$	$-\Delta G_{50}$
2	Linear	1	4.88 ± 0.33	2.58	3.13	2.07	4.85 ± 0.33	2.55	3.10	2.04
3	Ring	3	15.11 ± 0.89	9.38	11.27	7.98	15.14 ± 0.89	9.40	11.30	8.00
4	Ring	4	26.72 ± 1.75	18.06	20.93	15.61	26.56 ± 1.76	17.90	20.78	15.46
5	Ring	5	35.17 ± 2.42	24.30	27.65	20.97	34.90 ± 2.42	24.03	27.38	20.70
6	Cage	8	43.48 ± 2.98	30.52	34.29	26.14	44.45 ± 2.90	30.18	34.70	25.71
7	Prism34	10	55.24 ± 3.66	37.89	43.39	32.35	55.85 ± 3.66	38.50	44.00	32.96
8	D_{2d}	12	70.06 ± 4.68	48.68	55.75	41.84	70.86 ± 4.68	49.44	56.54	42.64
9[a]	Prism45	9	79.14 ± 5.39	55.69	63.27	48.05	82.00 ± 5.39	57.96	65.55	50.26
10[a]	Prism55	10	90.07 ± 6.13	63.48	72.14	54.74	93.42 ± 6.13	66.18	74.83	57.37
11[a]	Prism56	11	98.67 ± 6.82	69.66	78.99	59.98	102.14 ± 6.82	72.40	81.73	62.65
12[a]	Prism444	12	112.59 ± 7.5	79.41	90.13	68.34	118.02 ± 7.54	84.6	94.78	72.99

Note. The thermodynamic corrections were made using the B3LYP/6-311++G** values. For $n \leq 8$, all the geometries were fully optimized, while for $n \geq 9$, the single-point energy calculations were carried out for MP2/TZ2P++ and MP2/aug-cc-pVDZ+(2*s*2p/2*s*) on the MP2/TZ2P optimized geometries.

octamer ring conformers have similar red-shifts. These red-shifted values with respect to those of water monomer reflect the strength of H-bond interactions between water molecules. The cyclic pentamer cluster shows ~540 cm^{-1} red-shifted frequencies corresponding to "da" water, while the hexamer-Cage and heptamer-Prism34 show ~670 and ~760 cm^{-1} red-shifted frequencies, respectively, corresponding to "daa"-type water (Fig. 4, Table IV). The large shifts are due to the strong polarization effect by the H-bonds.

HOH bending modes of neutral water clusters display blue shifts with respect to that of the pure water monomer (Table IV). In going from "da" to "dda"-type water, the blue-shift increases. For mono-cyclic ring structures, the maximum blue-shifts of HOH bending modes

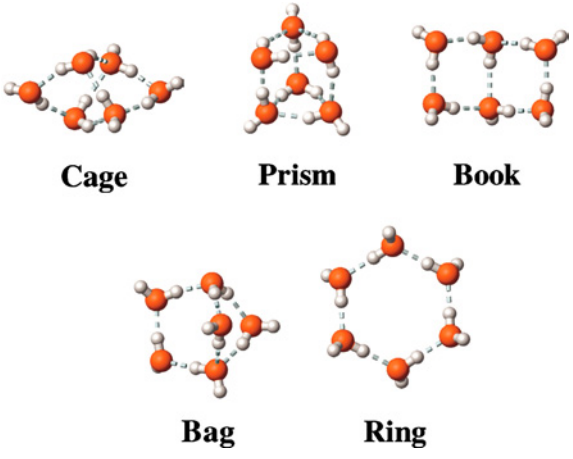

Fig. 3. Five isoenergetic isomers of neutral water hexamer.

of "da" waters increase from the cyclic trimer to pentamer; however, the hexamer to octamer show blue-shifts similar to the pentamer. The "dda" waters in the cage hexamer and cage heptamer and cubic D_{2d} conformers show the largest blue-shifts (~120 cm^{-1}) for the bending modes.

The order of red-shifts of OH stretching frequencies with respect to the average value of ν_3 and ν_1 of the water molecule in the water dimer to dodecamer is "da" (ν_3) < "daa" (ν_3) < "dda" (ν_3) < "ddaa" (ν_3) < "ddaa" (ν_1) ≈< "dda" (ν_1) < "da" (ν_1) < "daa" (ν_1). The IR intensities of double proton donor-type waters ("dda" and "ddaa") in asymmetric OH stretching modes (ν_3) are strong, while the intensities of single donor-type waters ("da" and "daa") are strong in symmetric OH stretching modes (ν_1). The order of red-shifts of bending frequencies with respect to that of monomer is "ddaa" > "dda" > "daa" ≈ "da." In the cases of undecamer and dodecamer, the ranges of $-\delta\nu_3$ and $-\delta\nu_1$ of "ddaa"-type are 209–299 and 245–496 cm^{-1}, and that of $\delta\nu_2$ of "ddaa"-type is 93–135 cm^{-1}. The values of $-\delta\nu_3$ and $-\delta\nu_1$ of "dda"-type are 66–242 and 181–436 cm^{-1} and that of $\delta\nu_2$ of "dda"-type is 46–138 cm^{-1}.

H-BONDS IN HYDRATION AND COORDINATION CHEMISTRY

As shown in Fig. 5, a hydroxide ion forms tetrahydrated structure using three lone pairs. The tetrahydrated fluoride ion has a surface state near 0 K, but as temperature increases to the room temperature, it can have nearly internal structure with tetrahedral coordination using four lone pairs of electrons due to

Table III. Interaction Energies (kcal/mol) of Five Isoenergetic Isomers of Neutral Water Hexamers[a]

Methods	$-\Delta E$	Ring	Book	Bag	Cage	Prism
MP2/QZ(3*df*/2*pd*)++	$-\Delta E_e$	43.34	44.04	43.40	44.21	44.23
MP2/HZ4P(2*fg*/2*d*)++	$-\Delta E_e$	43.89	44.73	44.10	45.02	45.13
MP2/CBS	$-\Delta E_e$	44.8	45.6	—	45.8	45.9
MP2/aug-cc-pVDZ + (2*s*2*p*/2*s*)[b]	$-\Delta E_0$	29.75	30.25	29.95	30.17	30.08
MP2/TZ2P	$-\Delta E_0$	31.67	32.17	31.44	32.17	31.98
MP2/QZ(3*df*/2*pd*)++	$-\Delta E_0$	29.64	30.00	29.34	29.94	29.65
MP2/HZ4P(2*fg*/2*d*)++[c]	$-\Delta E_0$	30.19	30.70	30.10	30.76	30.54

[a] All data were from reference 18 except MP2/aug-cc-pVDZ+(2*s*2*p*/2*s*) cases.
[b] The B3LYP/6-311++G** ZPEs were used for the ZPE correction.
[c] The MP2(FC)/6-311++G** ZPEs were used for the ZPE correction.

the entropy effect [12]. On the other hand, the tetrahydrated chloride ion has a surface bound state even at room temperature [12]. Strongly electronegative small ions form strong H-bonds with water molecules, which is larger than the water–water binding energy, due to the strong electrostatic interactions. While a cation has very strong electrostatic interaction, an anion has slightly weaker electrostatic interaction because the presence of an excess electron requires a large space for stabilization (i.e., lowering the kinetic energy of the excess electron).

COOPERATIVE EFFECT IN SHORT H-BOND

Although, in general sense, the cooperativity applies to all intermolecular interactions, it is particularly important in H-bond interaction because of the relay effect of hydrogen atoms. The H-bond distance tends to decrease as cluster size increases. A number of books and articles have been devoted to elucidate the cooperative effects in hydrogen bond [1, 2]. The typical characteristics of cooperative effects are the shorter X–H distance, longer X—H distance, larger chemical shift, and red shifts of the O—H vibrational spectra. In the following section, after reviewing previous work on linear hydrogen-bonded chains, we will discuss the nature of recently synthesized calix [4] hydroquinone (CHQ) nanotubes. Some of the questions we would like to address are the following: (1) how significantly bond distances and bond energies change in an infinite linear hydrogen-bonded chain? (2) what is the origin of these cooperativity? (3) what is the role of cooperativity in determining the structures of organic and biological molecules?

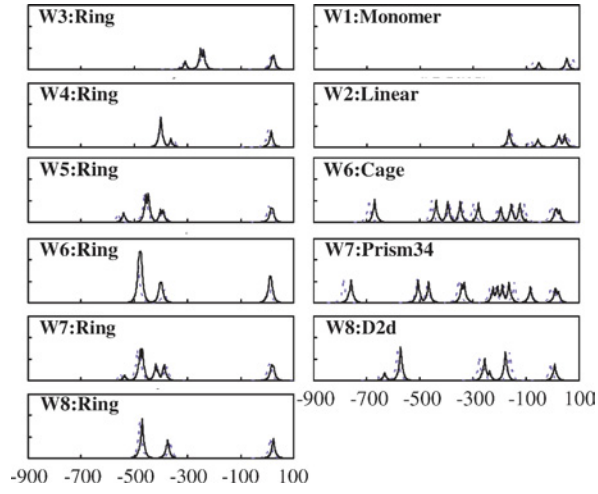

Fig. 4. B3LYP/6-311++G** (in solid line) and MP2/DZP (in dotted line) IR spectra for O—H stretch frequency shifts with respect to the average value of the free O—H symmetric and asymmetric stretch frequencies of the water monomer for the neutral water clusters, W_{1-8}.

Linear H-Bonded Chains

A number of studies have been devoted to investigate the property of linear H-bonded chains such as HF, HCN, and H_2O systems. Mostly, the HF dimer has been served as a hydrogen bond model. Experiments show that the bent dimer and cyclic hexamer are stable in cluster form. In crystalline hydrogen fluoride, HF forms infinite chain structure by strong hydrogen bond (F···F distance of 2.47 Å which is ∼0.25 Å shorter than the normal F···F distance of 2.72 Å in the finite system HF···HF) [24]. Guedes *et al*. have investigated the characteristics of cyclic HF and HCl clusters [25], and showed that hydrogen-bond cooperativity is related to electronic sharing and delocalization through electron density difference. Rincon *et al*. also showed that the cooperative effect is related to electron delocalization between monomer units through the analysis of the topology of electron density [26]. In addition, agreeing with the experimental result,

Table IV. B3LYP/6-311++G** Vibrational Frequency Shifts (With Respect to the Monomer Frequencies ν_3, ν_1, and ν_2) and IR Intensities (Average in Parentheses) of $(H_2O)_{n=2-8}$

		$-\delta\nu_3$			$-\delta\nu_1$			$\delta\nu_2$		
n	Conformation	"da"	"daa"	"dda"	"dda"	"da"	"daa"	"dda"	"daa"	"da"
2	Linear		"a": 8 (85)	"d": 30 (80)	"a": 3 (16)		"d": 112 (333)	"d": 26 (35)	"a": 10 (88)	
3	Ring	27–33 (79)				188–257 (372)				49–21 (63)
4	Ring	37–38 (69)				310–442 (738)				79–29 (52)
5	Ring	32–39 (67)				339–488 (894)				94–39 (51)
6	Ring	36–37 (67)				344–499 (974)				95–35 (54)
	Book	34–38 (68)	47 (77)	199 (398)	235 (320)	253–473 (1002)	552 (275)	115 (36)	79 (46)	60–26 (68)
	Bag	28–45 (75)	47 (52)	257 (675)	200 (576)	176–539 (791)	611 (398)	116 (56)	70 (86)	99–29 (53)
	Cage	26–45 (75)	39–43 (69)	176–208 (358)	143–226 (320)	295–342 (599)	385–617 (761)	106–93 (44)	73–57 (66)	38–32 (88)
	Prism	26–37 (70)	38–41 (70)	147–190 (256)	122–260 (364)		275–639 (592)	123–75 (76)	51–28 (91)	
7	Prism34	31 (64)	39–42 (70)	137–242 (387)	155–280 (367)	414 (623)	289–707 (787)	121–96 (51)	63–33 (67)	37 (151)
	Ring	28–39 (66)				334–484 (984)				98–41 (54)
8	D_{2d}		44 (63)	230–275 (555)	185–204 (206)		519–604 (885)	122–75 (24)	48–36 (101)	
	Ring	29–30 (67)				323–472 (1006)				94–39 (55)

Note. For $n = 1$, $\nu_3 = 3921\,(57)$, $\nu_1 = 3816(9)$, and $\nu_2 = 1603\,(67)$. Frequencies are in cm^{-1}; IR intensities in km/mol. If $\delta\nu_1 = \delta\nu_3$, it means that ν_1 is smaller than ν_3 by 105 cm^{-1}.

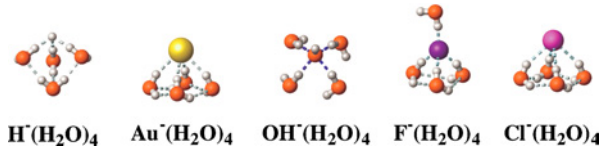

Fig. 5. Structures of tetra-hydrated anions.

they showed that the cyclic hexamer is the most favorable structure among cyclic clusters.

Hydrogen cyanide (HCN) has fully linear structure as both a dimer complex and a solid state conformer. Two different structures, cyclic and linear conformers, have been confirmed experimentally in the trimer cluster. Karpfen investigated the structures, binding energies and vibrational spectra of linear and cyclic HCN clusters, and concluded that HCN clusters have weaker cooperativity than HF [27].

Cooperative effects in H_2O appears as gradual shortening of hydrogen bond distance from dimer (2.98 Å) to liquid (∼2.8 Å) to ice (∼2.75 Å) [28]. Beside the studies of liquid water and ice, a lot of theoretical studies have been devoted to water chains [29–31]. Suhai calculated the bond distance and average H-bond energy in infinite water chain as 2.73 Å and 6.30 kcal/mol, respectively, which is comparable to experimental results on ice (2.74 Å, and 6.7 kcal/mol) [29]. Hermansson *et al.* investigated the polarization of the individual water molecules in finite and infinite H-bonded chains, and showed that the induced dipole moment in the middle of the long chain is about twice as large as those at the ends. The additional dipole moments are created by charge transfer from accepter to donor [30]. Masella *et al.* investigated the cooperative effects in cyclic trimers comprised of water and methanol [31].

Short H-Bond in Organic Crystal and Peptide Structures

The cooperativity of H-bond plays an important role in determining the structures of molecular crystals and biological molecules. Cyclohexane-1,3-dione forms sheet, which has long chains of hydrogen bond with most solvents (forms 6:1 cocrystal with benzene) [32]. Dannenberg *et al.* [33] explained this by comparing asymptotic interaction energy of the infinite chain and cyclic hexamer. Comparing differences between urea and 1,3-cyclohexanedione under external electric field, they found that the short distance in urea is reasonably described by electrostatic interaction and polarization effects, but 1,3-cyclohexanedione is not.

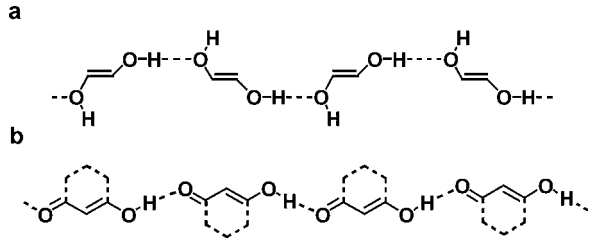

Fig. 6. Schematic of 1-D H-bonds relays. (a) 1-D H-bond relay of poly 1,2-ethanediols (diols). (b) 1-D H-bond relay of poly 1,3-propanedione (diones).

Cooperative effects in secondary protein structures, helix and sheet have been reported [34]. The linear chain of formamide which resembles peptides, has large cooperativity in H-bond, which is 2.5 times as much as that of formamide dimer. For the parallel and antiparallel sheet in secondary protein structures, there was no cooperativity in the parallel direction, while significant cooperativity exists in perpendicular direction. In methanol solvent system, the cooperative effects were reduced, indicating that the cooperativity is due to polarization effect.

Diol and Dione

We considered two different linear chainlike H-bond relay, poly 1,2-ethanediols and 1,3-propanedione (Fig. 6) [35]. We have optimized the geometries on the plane up to the decamer at the B3LYP/6-31G* level, and up to hexamer at the MP2/6-31G* level. We obtained the binding energy of infinite chain on the basis of the exponential decay plot (Fig. 7).

In the case of the dimer, 1,3-propanedione has larger H-bond energy (12.3 kcal/mol) than 1,2-ethanediol (5.9 kcal/mol) at the B3LYP level. Based on the exponential decay plot, the H-bond energies in the infinite chains of 1,3-propanedione and 1,2-ethanediol are 24.4 and 9.8 kcal/mol, respectively, which increased by 12.0 and 3.9 kcal/mol, respectively, than those of the dimers (Fig. 7). Also, bond distances are shortened by 0.07 and 0.15 Å, respectively. MP2 results are comparable with B3LYP results. Change of natural bond orbital (NBO) atomic charge (Fig. 7) shows that the polarization is mainly responsible for this cooperativity. H-bond between diones is stronger with the larger cooperativity effect than that of diols.

Short H-Bond for Organic Nanotubes and the Solvent Effect

We recently synthesized calix[4]hydroquinone (CHQ) nanotubes, which are assembled by

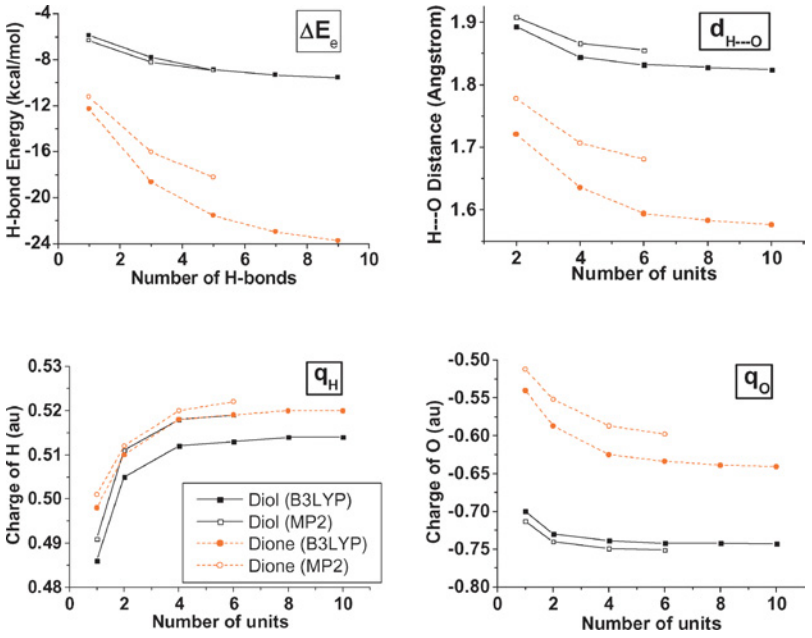

Fig. 7. ZPE-uncorrected H-bond interaction energies (ΔE_e), H···O distances ($d_{H\cdots O}$), and atomic charges of H and O atoms of the central H-bond (q_H, q_O) in the 1-D H-bond relay of 1,2-ethanediols and 1,3-propanediones. Reproduced by permission of American Chemical Society: Reference [35] Suh, S. B.; Kim, J. C.; Choi, Y. C.; Yun, S.; Kim, K. S. *J. Am. Chem. Soc*. **2004**, *126,* 2186.

one-dimensional (1-D) short hydrogen bond (SHB) (Fig. 8) [4]. Hydrogen bond length in CHQ is about 2.65 Å , which is almost 0.2 Å shorter than that of normal hydrogen bond. For cluster systems, we have carried out B3LYP and MP2 calculations. To investigate the periodic systems including solvent, we have carried out plane wave density functional theory (PW-DFT) using generalized gradient approximation (GGA) of Perdew and Wang [36], and the Vanderbilt pseudopotentials [37].

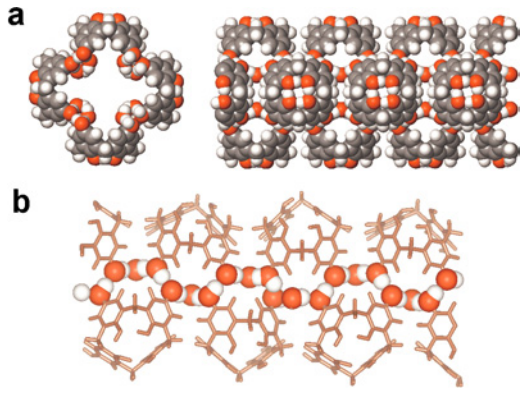

Fig. 8. Longitudinal H-bond relay comprised of CHQs and water. (a) Tubular polymer structure of a single nanotube obtained with X-ray analysis for the heavy atoms and with *ab initio* calculations for the H orientations (top and side views). (b) One of four pillar frames of short H-bonds represents a 1-D H-bond relay composed of a series of consecutive OH groups [hydroxyl groups (—OH) in CHQs and the OHs in water molecules]. Reproduced by permission of American Chemical Society: Reference [35] Suh, S. B.; Kim, J. C.; Choi, Y. C.; Yun, S.; Kim, K. S. *J. Am. Chem. Soc*. **2004**, *126,* 2186.

One-dimensional SHB in CHQ nanotubes involve three kinds of H-bond between hydroquinone (Q_h) and water (W). We denote the complex with a H-donor and a H-acceptor as D > A. The W > Q_h, Q_h > Q_h, and Q_h > W in Fig. 9 have bond energies of 5.4, 6.3, 8.6 kcal/mol, respectively (B3LYP/6-31G*). These values are similar to MP2/6-31G* results of 5.6, 7.8, and 8.5 kcal/mol and PW-DFT results of 5.6, 4.6, and 8.4 kcal/mol. Case Q_h > W has ∼0.15 Å shorter O···H bond distance and ∼3 kcal/mol larger binding energy than case W > Q_h. From orbital interpretation of hydrogen bond, an H atom is likely to stabilize the lone pair electrons of water oxygen atom more than those of hydroquinone oxygen atom.

In order to investigate the effect of SHB in CHQ nanotubes, we have performed calculations with the increasing number of H-bonded clusters. On the basis of exponential decay plot, the asymptotic H-bond energies for W > Q_h, Q_h > Q_h, and Q_h > W in infinite H-bond relay are estimated to be 11, 11, and 12 kcal/mol, respectively. The average value of these H-bond energies is

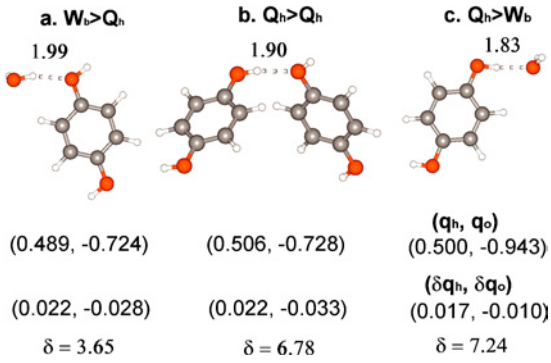

Fig. 9. Three types of H-bonding involved with 1-D H-bonds of CHQ nanotubes. The H···O bond distances (Å), atomic charges (q_H and q_O in au) and their changes with respect to the values of the isolated systems (Δq_H and Δq_O in au), and proton chemical shifts (δ in ppm) are given at the B3LYP/6-31G* level.

11.3 kcal/mol, which is 4.5 kcal/mol higher than the normal H-bond.

We have calculated the average bond energy gain in the infinite SHB array (E_{shb}) and the solvent effect in bond energy (E_{sol}) using the partition scheme. In this case, E_{shb} is −3.9 kcal/mol, and E_{sol} is 1.2 kcal/mol. Thus average HB energy per SHB in the presence of solvent water molecule is 8.9 kcal/mol, which is 2.7 kcal/mol larger than normal H-bond energy.

SHORT STRONG H-BOND IN ENZYME CATALYSIS

Short strong H-bond (SSHB) [38, 39] is characterized by their large hydrogen bond energies (>10 kcal/mol), short distances (<2.6 Å), and large downfield shift of NMR resonances (>15 ppm). In low dielectric organic solvents, unusual physicochemical properties have been observed for a number of hydrogen bonds between two partners with an equal pK_a.

The proposal that SSHB plays a key role in the enzymatic catalysis has been highly debated in recent years [40]. One of the examples for the role of SSHB in enzymatic reaction can be found in Δ^5-3-Ketosteroid Isomerase (KSI) which is a paradigm for fast enzymatic reactions [41]. KSI catalyzes the conversion of β,γ- to α,β-unsaturated steroidal ketones via a dienolate intermediate at a nearly diffusion-controlled rate. During the reactions, Asp38 serves as a base for abstracting the C4β-proton of the steroid substrate, while Tyr14 (H-bonded by Tyr55) and Asp99 serve as catalytic residues by providing H-bonds to the oxyanion (C3—O or O3) of the dienolate intermediate (Fig. 10).

The calculated results about energy profile of the wild-type system [38] indicates that the barriers for the first step (ES → TS1 → EI1; abstraction of the proton from the substrate) and the third step (EI2 → TS3 → EP; donation of the proton to the substrate) are very similar and crucial in energy, while the second step (EI1 → TS2 → EI2; rotation of Asp38) is not significant in energy so that total reaction is eventually two-step mechanism. In the presence of Tyr14 or Asp99, the transition states TS1 and TS3 are lowered by ∼6 kcal/mol. This result implies that the catalytic effect of the two residues is almost equivalent. When Tyr14 and Asp99 were introduced simultaneously, TS1 and TS3 are lowered by ∼10 kcal/mol. Intermediate states (EIs: EI1 and EI2) and TS2 are stabilized by ∼15 kcal/mol, suggesting that the two functional groups contribute cooperatively to the stabilization of EIs and TS2.

In the structure of the active sites in the complex with the intermediate analogues, the hydrogen bond distances between O3 and Tyr14 or Asp99 are ∼2.6 Å, which is slightly shorter than those (∼2.8 Å) of the structure in complex with the product analogue [38] (Table V). NMR spectroscopic investigations also indicate that in the D38N mutant KSI, the H-bond between the catalytic residues and equilenin exhibits a large downfield shifted peak (>16 ppm) [41, 42].

The distances between $O_{residue}$ and O3 ($d[O_r—O3]$) along the reaction path (Table V) [38] indicates that even though normal H-bonds are formed between residues and substrate at the starting and ending point of reaction, they are converted to short strong one during the reaction where $d[O_r—O3]$ is reduced by ∼0.2 Å, in accordance with the experimental results.

π-TYPE H-BOND

The comparison of π-type H-bond interaction and traditional water-water σ-type H-bond interaction should be very interesting. The interaction energies of ethylene–water π-H bond and water–water σ-H bond interactions were calculated to be 2.84 ± 0.59 and 4.89 ± 0.41 kcal/mol at the MP2/aug-cc-pVDZ level, where the lower and upper limits are the BSSE-corrected and -uncorrected values, respectively. In order to analyze the interaction energy component, the symmetry-adapted perturbation theory (SAPT) [43] calculations were performed using the same basis set and geometries. SAPT have been used to analyze the interaction energies as the terms of electrostatic, induction, dispersion, and exchange interaction components:

$$E_{int}^{(SAPT)} = E_{elst}^{(1)} + E_{exch}^{(1)} + E_{ind}^{(2)} + E_{exch-ind}^{(2)} + E_{disp}^{(2)} + E_{exch-disp}^{(2)} + \delta_{int}^{(HF)},$$

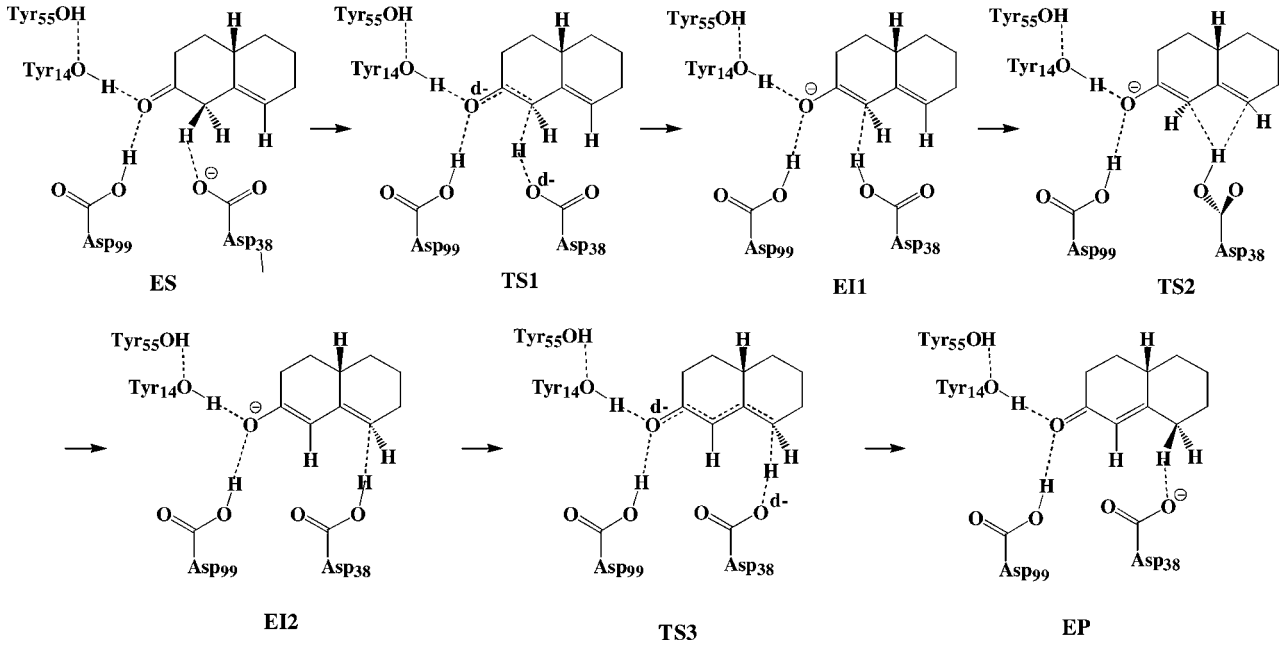

Fig. 10. Schematic representation of reaction mechanism of KSI.

where $E^{(1)}_{\text{elst}}$ is the electrostatic interaction energy of the monomers with the unperturbed electron distribution, $E^{(1)}_{\text{exch}}$ their first-order valence repulsion energy due to the Pauli exclusion principle, $E^{(2)}_{\text{ind}}$ stands for the second-order energy gain resulting from the induction interaction, $E^{(2)}_{\text{exch-ind}}$ represents the repulsive exchange interaction due to the electronic cloud deformation, $E^{(2)}_{\text{disp}}$ indicates the second-order dispersion energy, $E^{(2)}_{\text{exch-disp}}$ denotes the second-order correction for a coupling between the exchange repulsion and the dispersion interaction, and $\delta^{\text{HF}}_{\text{int}}$ includes the higher-order correction for the induction and the exchange interactions.

For the ethene–water and water–water SAPT interaction energies without ZPE correction (ΔE_{e}; −2.0 and −4.1 kcal/mol, respectively), the electrostatic components are −3.9 and −8.4 kcal/mol, the first-order exchange components are 5.5 and 8.5 kcal/mol, the second-order induction terms are −2.7 and −2.9 kcal/mol, and the second-order dispersion energies are −2.4 and −2.3 kcal/mol, respectively. The electrostatic interaction is dependent on the electronegativity difference between H-bond component atoms, which is available in the water–water H-bond interaction. The π systems have low energy lowest-energy unoccupied molecular orbitals (LUMOs) and polarizable π electrons occupied in the higher energy molecular π orbitals. The π systems can play a role of good electron-donating group. Therefore, with respect to the electrostatic interaction energy of π H-bond interaction, the exchange component is highly repulsive. While the exchange component of water–water H-bond interaction is in the magnitude similar to the electrostatic interaction, the induction energy of π-H-bond interaction has relatively large energy component. The dispersion interaction is also relatively large due to the diffuse and polarizable π electron density in the π-H bond interaction.

Table V. Distances (Å) Between O_{residue} and O3 Along the Reaction Path (Fig. 10) in Wild-Type of KSI

Residue	ES	TS1	EI1	TS2	EI2	TS3	EP
Tyr14	2.68	2.64	2.55	2.51	2.55	2.61	2.67
Asp99	2.75	2.66	2.60	2.55	2.58	2.65	2.71

H-BOND IN RECEPTORS/IONOPHORES

Host–guest complexes play an important role in biological processes, and H-bonds play a crucial role in the molecular recognition phenomena. In this context, by utilizing hydrogen bond interaction, various ionophores/receptors with selective binding affinity of specific ions have been designed, and demonstrated by experiments [6, 13, 44–46]. Usually, H-bonds in those receptors are in competition with the interaction of polar solvent with ions. Therefore, the most important strategy in designing receptors/ionophores is to know how

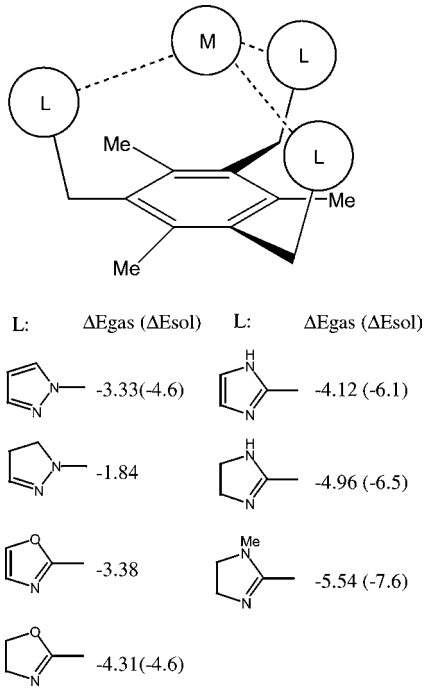

Fig. 11. Relative affinities (kcal/mol) of various ammonium receptors for NH_4 over K^+. ΔE_{sol} for selected receptors in $CHCl_3$ solution were obtained using the IPCM method.

to optimize the H-bond between receptor and ion in the presence of solvent molecules.

H-Bond in the Selective Receptor for Ammonium Ion (NH_4^+) Over Potassium Ion (K^+)

The recognition of NH_4^+ has attracted lots of interest since ammonium-containing compounds are very important in chemical, biological, and physiological molecular system [44]. One of the major problems in the selective recognition of NH_4^+ over K^+ arises from their nearly equivalent sizes. Since the pK_a of NH_4^+ is 9.0, the subunit to recognize NH_4^+ should be strong proton-withdrawing to strengthen the charged H-bonds [47]. Figure 11 shows the interaction energies in the gas phase and CH_3Cl_3 solution for the tripodal receptor with various subunits to selectively recognize NH_4^+ over K^+. The interaction energy in solvent was calculated using the static isodensity surface polarized continuum model (IPCM) method.

Apart from the recognition efficacy in solvent, the receptors need to possess solvent access-blocking groups (such as Me). In this way, the coordination number of the receptors is limited to no more than 4. Since NH_4^+ and K^+ favor the coordination numbers of 4 and 6, respectively [48], the optimally solvated NH_4^+ in the presence of receptors is more energetically favored than the undersolvated K^+.

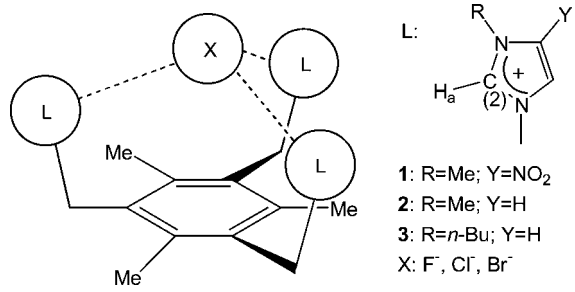

Fig. 12. Schematics of tripodal receptors for halide ions.

Ionic H-Bonds in Receptors for Anions

With an aid of supramolecular chemistry, recognizing and sensing anionic species have recently emerged as a key research field [6, 13, 44–46]. In particular, the development of receptors capable of selectively recognizing a specific anion is quite intriguing. To enhance the sensing efficacy and selectivity of anions in solvent, strong ionic H-bond has been frequently harnessed. In this vein, several selective receptors utilizing charged H-bonds will be introduced.

Recently, we have designed the tripodal receptors (**1–3**) with 1,3-disubstituted imidazolium ring subunit which can form $(C–H)^+\cdots X^-$ hydrogen bonds with anions [6] (Fig. 12), in contrast with the common practice that most positively charged anion receptors were designed to form $N—H\cdots X^-$ hydrogen bonds. ^1H NMR titration experiment was performed to investigate anion binding properties of hosts. Upon addition of chloride anion to host **1**, significantly large down field shifts ($\Delta\delta > 0.94$ ppm) were observed for the proton of C(2) which is in between two N atoms of imidazolium subunit. This suggests complexation of the anion by CH hydrogen bonds. Although both hosts **1** and **2** show higher affinities for the chloride anion than bromide, the affinity and the selectivity of host **1** for halide anions are much higher than those of host **2** (Table VI). This is a consequence of stronger $(C—H)^+\cdots X^-$ hydrogen bonds by more electron-deficient imidazolium moieties as well as more enhanced charge-dipole interaction by the NO_2 group.

In spite of the enhanced affinity for halide anions, the recognition of F^- was not accomplished through charged H-bond with host **1**, because of the nucleophilic reaction of F^- on C(2). For the complex of host **2** and F^-, *ab*

Table VI. Association Constants (K_a) and Binding Free Energies (ΔG^0) for 1:1 Complexes of Host **1–3** (Fig. 12) with Anions in DMSO-d_6 at 298 K

Hosts	Anions	K_a (M^{-1})	$-\Delta G^0{}_{298}$
1	Cl^-	4800	5.02
	Br^-	490	3.67
2	F^-	1300	4.25
	Cl^-	1100	4.15
	Br^-	180	3.07
3	F^-	2400	4.61
	Cl^-	1500	4.33

Note. Estimated errors <10%. Anions used in this assay were in the form of their tetrabutylammonium salts. $-\Delta G^0{}_{298}$ is in kcal/mol.

initio calculations predicted that F^- forms shorter and more linear H-bond with host **2** than Cl^- or Br^-, so that F^- shows higher binding energies both in the gas and polar solvent phases. In polar solvent with dielectric constant of acetonitrile ($\varepsilon = 36.64$), the calculated binding energies of **2** with F^- and Cl^- decrease to only ~20 kcal/mol, while they are larger than 200 kcal/mol in the gas phase. This indicates that the cationic imidazolium receptor interacts with polar solvent so that its effective charges on C(2) diminish, and its ability of forming charged H-bond with anions decreases. This trend is confirmed again in the experimental results in 1:1 mixture of DMSO-d_6 and acetonitrile-d_3 or DMSO-d_6 solvent. In these highly polar solvent, F^- interacts moderately with host **3**, while the butyl groups block the direct interaction of F^- with solvent molecules and reduce the micro-environmental polarity around the binding site.

Recently, by extending this approach, a receptor of anthracene derivative with two imidazolium moieties which show selective binding affinity for $H_2PO_4^-$ over other halide anions and anion-induced changes in fluorescence was reported (host **4** in Fig. 13) [46]. However, further investigation shows that F^- forms 2:1 complex with receptor on each charged H-bonding site. In addition to $(C{-}H)^+\cdots F^-$ bonding (1.63 Å), due to the high flexibility of the receptor site of host **4**, the hydrogen atom connecting CH_2 between the anthracene and imidazolium moiety also interacts with F^- at a distance of 2.29 Å. On the other hand, host **5** favors $H_2PO_4^-$ over F^- in polar acetonitrile solvent. For both hosts **4** and **5** systems, their $H_2PO_4^-\cdots(H{-}C)^+$ distances are almost same, and so are $F^-\cdots(H{-}C)^+$ distances (1.7 and 1.6 Å, respectively). In the case of host **5**, however, $F^-\cdots(H_2C)$ interaction becomes negligible (>3 Å). Consequently, the greater rigidity of host **5** enhances the binding selectivity towards $H_2PO_4^-$.

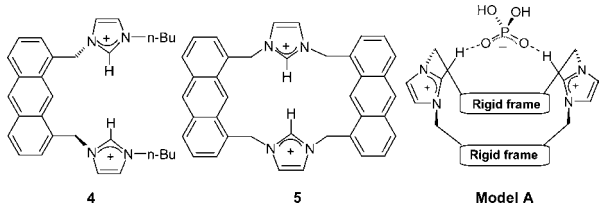

Fig. 13. Molecular system (model A) designed for the recognition of $H_2PO_4^-$. Reproduced by permission of American Chemical Society: Reference [46(b)] Yoon, J.; Kim, S. K.; Singh, N. J.; Lee, J. W.; Yang Y. J.; Chellappan, K.; Kim, K. S. *J. Org. Chem.* **2004**, *69,* 581.

H-Bond in Amphi-Ionophores

Cyclic polypeptides [49] can interact with both cations through C═O moieties and anions through N─H moieties (Fig. 14). In structures **6** and **7**, both carbonyl and amide groups are nearly on the same cylindrical surface, i.e., nearly parallel to the principal axis. Upon complexation with an ion, the cyclic peptides are found to have two types of binding: one at center ($\mathbf{n}'{\cdot}\mathbf{I}$ where **n** denotes the cyclic peptides and **I** denotes an ion) and the other above the molecular plane ($\mathbf{n}'{\cdot}\mathbf{I}$). In the presence of cation, carbonyl dipole moieties tend to point

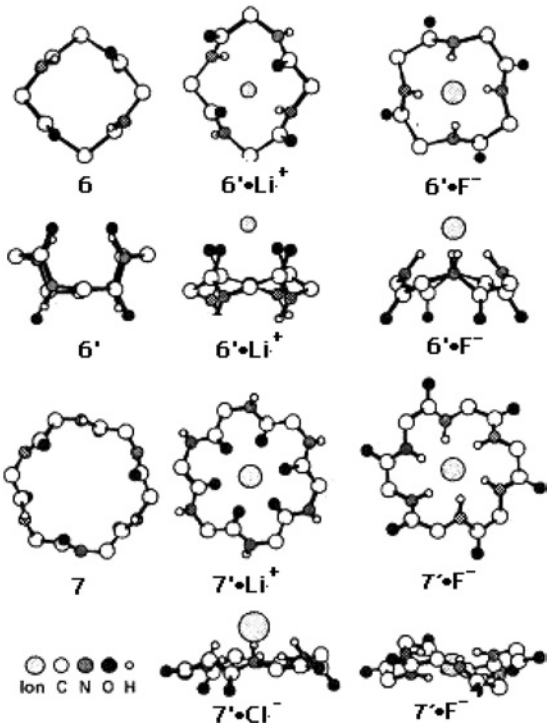

Fig. 14. Selected structures of cyclic peptides (glycine) and their ion complexes. Reproduced by permission of American Chemical Society: Reference [49(a)] Kim, K. S.; Cui, C.; Cho, S. J. *J. Phys. Chem. B* **1998**, *102,* 461.

inward (toward the cation), while, in the presence of an anion, amide dipole moieties point inward, forming H-bond. The type of binding is decided by the size of ions and the cavity of cyclic peptides. If an ion is small and the cyclic peptides is sufficiently large, then **n**·**I**-type complex is formed. Otherwise, **n**′·**I**-type complexation is observed. When **7** binds with F^-, it prefers **n**·**I**-type binding. In the case of Cl^-, however, the complex changes its geometry to **n**′·**I**. In **7**′·**Cl**$^-$, the $Cl^- \cdots H$ distances are 2.57 Å for three H atoms and 2.68 Å for the remaining three H atoms with supplementary angle, ϕ, equal to 30 and 37°, respectively.

CONCLUDING REMARKS

The most simplest and abundant atom in the universe, hydrogen atom is involved in one of the most complex and flexible bonding in both chemical and biological systems, giving its special features including wide range interaction energies, cooperativity effect, proton exchange through the H-bonds, self assembly of molecular tubes and layers, and functional geometries of multiply H-bonded frames in biological molecules. We have illustrated how a variety of different chemical systems have different H-bonding characteristics, and how each energy component plays in these bonds. Normally, the good proton-accepting and proton-donating capability and the dipole give combinatorially strong H-bond interactions. Many N-containing H-bond interaction systems in biochemical systems should be considered more in regard to biochemical-solvation phenomena. The studies of these weak interaction systems could be applied to the developments of available functional molecular systems. Indeed, utilizing the cooperative versus competitive effect of hydrogen bonds, we have been successful in designing various hydrogen-bonded ionophores, receptors, supramolecules, nanomaterials, and nanodevices [50]. Therefore, we hope that the present review of the H-bonding would be useful for understanding the role of H-bonding in molecular and biomolecular systems.

ACKNOWLEDGMENTS

This research was supported by KOSEF(CRI) and partly by BK21.

REFERENCES

1. (a) Jeffrey, G. A.; Saenger, W. *Hydrogen Bonding in Biological Structures*; Berlin: Springer-Verlag, 1991; (b) Jeffrey, G. A. In *An Introduction to Hydrogen Bonding*; Truhlar, D. G., Eds.; Oxford University Press: New York, 1997.
2. (a) *Modeling the Hydrogen Bond in ACS Symposium Series 569*; Smith, D. A., Ed.; American Chemical Society: Washington, DC, 1994; (b) Scheiner, S. In *Hydrogen Bonding. A Theoretical Perspective*; Oxford University Press: New York, 1997; (c) Desiraju, G. R.; Steiner, T. D. In *The Weak Hydrogen Bond: In Structural Chemistry and Biology (International Union of Crystallography Monographs on Crystallography, 9)*; Oxford University Press: New York, 1999.
3. (a) Tarakeshwar, P.; Kim, K. S. In *Encyclopedia of Nanoscience and Nanotechnology*; Nalwa, H. S., Ed.; American Science Publishers: California, 2004; Vol. 7, pp. 367–404; (b) Schmidtchen, F. P.; Berger, M. *Chem. Rev*. **1997,** *97*, 1609; (c) Tarakeshwar, P.; Choi, H. S.; Kim, K. S. *J. Am. Chem. Soc*. **2001,** *123*, 3323; (d) Auer, F.; Schubert, D. W.; Stamm, M.; Arnebrant, T.; Swietlow, A.; Zizlsperger, M.; Sellergren, B. *Chem. Eur. J*. **1999,** *5*, 1150; (e) Kim, H. G.; Lee, C.-W.; Yun, S.; Hong, B. H.; Kim, Y.-O.; Kim, D.; Ihm, H.; Lee, J. W.; Lee, E. C.; Tarakeshwar, P.; Park, S.-M.; Kim, K. S. *Org. Lett*. **2002,** *4*, 3971; (f) Wulff, G.; Gross, T.; Schonfeld, R. *Angew. Chem. Int*. **1997,** *36*, 1962; (g) Sukharevsky, A. P.; Read, I.; Linton, B.; Hamilton, A. D.; Waldeck, D. H. *J. Phys. Chem. B* **1998,** *102*, 5394.
4. (a) Hong, B. H.; Lee, J. Y.; Lee, C.-W.; Kim, J. C.; Bae, S. C.; Kim, K. S. *J. Am. Chem. Soc*. **2001,** *123*, 10748; (b) Hong, B. H.; Bae, S. C.; Lee, C.-W.; Jeong, S.; Kim, K. S. *Science* **2001,** *294*, 348; (c) Kim, K. S.; Suh, S. B.; Kim, J. C.; Hong, B. H.; Tarakeshwar, P.; Lee, J. Y.; Kim, Y.; Yun, S.; Lee, E. C.; Ihm, H. J.; Kim, H. G.; Lee, J. W.; Kim, J. K.; Lee, H. M.; Kim, D.; Cui, C.; Lee, J. W.; Youn, S. J.; Kim, C. Y.; Chung, H. Y.; Choi, H. S.; Lee, C.-W.; Cho, S. J.; Jeong, S.; Cho, J.-H. *J. Am. Chem. Soc*. **2002,** *124*, 14268; (d) Suh, S. B.; Hong, B. H.; Tarakeshwar, P.; Youn, S. J.; Jeong, S.; Kim, K. S. *Phys. Rev. B* **2003,** *67*, 241402(R).
5. (a) Mittal, R.; Howard, A. *Phys. Rev. B* **1996**, *53*, 14171; (b) Mei, H. S.; Tuckerman, M. E.; Sagnella, D. E.; Klein, M. L. *J. Phys. Chem. B* **1998,** *102*, 10446.
6. Yun, S.; Ihm, H.; Kim, H. G.; Lee, C.-W.; Indrajit, B.; Oh, K. S.; Gong, Y. J.; Lee, J. W.; Yoon, J.; Lee, H. C.; Kim, K. S. *J. Org. Chem*. **2003,** *68*, 2467; Ihm, H.; Yun, S.; Kim, H. G.; Kim, J. K.; Kim, K. S. *Org. Lett*. **2002,** *4*, 2897.
7. (a) Kim, K. S.; Clementi, E. *J. Am. Chem. Soc*. **1985,** *107*, 5504; (b) Son, H. S.; Hong, B. H.; Lee, C.-W.; Yun, S.; Kim, K. S. *J. Am. Chem. Soc*. **2001,** *123*, 514.
8. (a) Kollman, P. A.; Allen, L. C. *Chem. Rev.* **1972,** *72*, 283; (b) Alkorta, I.; Rozas, I.; Elguero, J. *Chem. Soc. Rev.* **1998,** *27*, 163; (c) Hobza, P.; Havlas, Z. *Chem. Rev.* **2000,** *100*, 4253; (d) Wormer, P. E. S.; Avoird, A. V. D. *Chem. Rev.* **2000**, *100*, 4109; (e) Tarakeshwar, P.; Kim, K. S. *J. Mol. Struct*. **2002,** *615*, 227; (f) Tarakeshwar, P.; Lee, H. M.; Kim, K. S. In *Reviews of Modern Quantum Chemistry*; Sen, K. D., Ed.; World Scientific: Singapore, 2002; Vol. II, p. 1642; (g) Perrin, C. L.; Nielson, J. B. *Annu. Rev. Phys. Chem*. **1997,** *48*, 511.
9. Kim, K. S.; Tarakeshwar, P.; Lee, J. Y. *Chem. Rev*. **2000,** *100*, 4145.
10. (a) Odde, S.; Mhin, B. J.; Lee, S.; Lee, H. M.; Kim, K. S. *J. Chem. Phys*. **2004,** *120*, 9524; (b) Re, S.; Osamura, Y.; Suzuki, Y.; Schaefer, H. F., III, *J. Chem. Phys*. **1998,** *109*, 973; (c) Cabaleiro-Lago, E. M.; Hermida-Ramon, J. M.; Rodriguez-Otero, J. *J. Chem. Phys*. **2002,** *117*, 3160.
11. (a) Lee, H. M.; Tarakeshwar, P.; Park, J.; Kolaski, M. R.; Yoon, Y. J.; Yi, H.; Kim, W. Y.; Kim, K. S. *J. Phys. Chem. A* **2004,** *108*, 2949; (b) Kim, J.; Lee, S.; Cho, S. J.; Mhin, B. J.; Kim, K. S. *J. Chem. Phys*. **1995,** *102*, 839; (c) Lee, H. M.; Min, S. K.; Lee, E. C.; Min, J. H.; Odde, S.; Kim, K. S. *J. Chem. Phys*. **2005,** *122*, 064314.
12. (a) Blades, A. T.; Jayaweera, P.; Ikonomou, M. G.; Kebarle, P. *J. Chem. Phys*. **1990,** *92*, 5900; (b) Perera, L.; Berkowitz, M. L. *J. Chem. Phys*. **1993,** *99*, 4222; (c) Roeselova, M.; Jacoby, G.; Kaldor, U.; Jungwirth P. *Chem. Phys. Lett*. **1998,** *293*, 309; (d) Baik, J.; Kim, J.; Majumdar, D.; Kim, K. S. *J. Chem. Phys*. **1999,** *110*, 9116; (e) Majumdar, D.; Kim, J.; Kim, K. S. *J. Chem. Phys*. **2000,** *112*, 101; (f) Kim, J.; Lee, H. M.; Suh, S. B.; Majumdar, D.; Kim, K. S. *J. Chem. Phys*. **2000,** *113*, 5259; (g) Lee, H. M.; Kim, K. S. *J. Chem. Phys*. **2001**, *114*, 4461; (h) Masamura, M. *J. Chem. Phys*. **2002,** *117*, 5257; (i) Lee, H. M.; Kim, D.; Kim, K. S. *J. Chem. Phys*. **2002,** *116*,

5509; (j) Vila, F.; Jordan, K. D. *J. Phys. Chem. A* **2002,** *106*, 1391; (k) Odde, S.; Pak, C.; Lee, H. M.; Kim, K. S. *J. Chem. Phys.* **2004,** *121*, 204; (l) Grishina, N.; Buch, V. *J. Chem. Phys.* **2004,** *120*, 5217; (m) Lee, H. M.; Suh, S. B.; Tarakeshwar, P.; Kim, K. S. *J. Chem. Phys.* **2005,** *122*, 044309.

13. (a) Kwon, J. Y.; Singh, N. J.; Kim, H. N.; Kim, S. K.; Kim, K. S.; Yoon, J. Y. *J. Am. Chem. Soc.* **2004,** *126*, 8892; (b) Yun, S.; Kim, Y.-O.; Kim, D.; Kim, H. G.; lhm, H.; Kim, J. K.; Lee, C.-W.; Lee, W. J.; Yoon, J.; Oh, K. S.; Yoon, J.; Park, S.-M.; Kim, K. S. *Org. Lett.* **2003,** *5*, 471; (c) Manojkumar, T. K.; Kim, D.; Kim, K. S. *J. Chem. Phys.* **2005,** *122*, 014305; (d) Bandyopadhyay, I.; Lee, H. M.; Kim, K. S. *J. Phys. Chem. A* **2005,** *109*, 1720; (e) Lee, E. C.; Hong, B. H.; Lee, J. Y.; Kim, J. C.; Kim, D.; Kim, Y.; Tarakeshwar, P.; Kim, K. S. *J. Am. Chem. Soc.* **2005,** *127,* 4530.
14. (a) Lisy, J. M. *Int. Rev. Phys. Chem.* **1997,** *16*, 267; (b) Kim, K. S.; Lee, J. Y.; Choi, H. S.; Kim, J.; Jang, J. H. *Chem. Phys. Lett.* **1997,** *265*, 497; (c) Rodgers, M. T.; Armentrout, P. B. *J. Phys. Chem. A* **1997,** *101*, 1238; (d) Tarakeshwar, P.; Choi, H. S.; Lee, S. J.; Lee, J. Y.; Kim, K. S.; Ha, T.-K.; Jang, J. H.; Lee, J. G.; Lee, H. *J. Chem. Phys.* **1999,** *111*, 5838; (e) Tarakeshwar, P.; Kim, K. S.; Brutschy, B. *J. Chem. Phys.* **2001,** *114*, 1295; (f) Stace, A. J. *Science* **2001,** *294*, 1292; Stace, A. J. *Phys. Chem. Chem. Phys.* **2001,** *3*, 1935; (g) Tarakeshwar, P.; Choi, H. S.; Kim, K. S. *J. Am. Chem. Soc.* **2001,** *123*, 3323; (h) Tarakeshwar, P.; Kim, K. S.; Kraka, E.; Cremer, D. *J. Chem. Phys.* **2001,** *115*, 6018; (i) Stace, A. J. *J. Phys. Chem. A* **2002,** *106*, 7993; (j) Manojkumar, T. K.; Choi, H. S.; Tarakeshwar, P.; Kim, K. S. *J. Chem. Phys.* **2003,** *118*, 8681; (k) Subirana, J. A.; Soler-Lopez, M. *Annu. Rev. Biophys. Biomol. Struct.* **2003,** *32*, 27.
15. (a) Gora, R. W.; Roszak, S.; Leszczynski, *J. Chem. Phys. Lett.* **2000,** *325*, 7; (b) Grabowski, S. J.; Robinson, T. L.; Leszczynski, J. *Chem. Phys. Lett.* **2004,** *386*, 44; (c) Grabowski, S. J. *Chem. Phys. Lett.* **2001,** *338*, 361; (d) Melandri, S.; Sanz, M. E.; Caminati, W.; Favero, P. G.; Kisiel, Z. *J. Am. Chem. Soc.* **1998,** *120*, 11504.
16. (a) Lee, H. M.; Lee, S.; Kim, K. S. *J. Chem. Phys.* **2003,** *119*, 187; (b) Suh, S. B.; Lee, H. M.; Kim, J.; Lee, J. Y.; Kim, K. S. *J. Chem. Phys.* **2000,** *113*, 5273.
17. (a) Wang, Y.-S.; Chang, H.-C.; Jiang, J.-C.; Lin, S. H.; Lee, Y. T.; Chang, H.-C. *J. Am. Chem. Soc.* **1998,** *120*, 8777; (b) Jiang, J.-C.; Wang, Y.-S.; Chang, H.-C.; Lin, S. H.; Lee, Y. T.; Niedner-Schatteburg, G.; Chang, H.-C. *J. Am. Chem. Soc.* **2000,** *122*, 1398.
18. (a) Lee, H. M.; Suh, S. B.; Lee, J. Y.; Tarakeshwar, P.; Kim, K. S. *J. Chem. Phys.* **2000,** *112*, 9759; (b) Lee, H. M.; Suh, S. B.; Lee, J. Y.; Tarakeshwar, P.; Kim, K. S. *J. Chem. Phys.* **2001,** *114*, 3343; (c) Lee, H. M.; Suh, S. B.; Kim, K. S. *J. Chem. Phys.* **2001,** *114*, 10749; Lee, H. M.; Suh, S. B.; Kim, K. S. *J. Chem. Phys.* **2002,** *115*, 7331.
19. (a) Kim, K. S.; Dupuis, M.; Lie, G. C.; Clementi, E. *Chem. Phys. Lett.* **1986,** *131*, 451; (b) Mhin, B. J.; Kim, H. S.; Kim, H. S.; Yoon, J. W.; Kim, K. S. *Chem. Phys. Lett.* **1991,** *176*, 41; (c) Kim, K. S.; Mhin, B. J.; Choi, U.-S.; Lee, K. *J. Chem. Phys.* **1992,** *97*, 6649; (d) Mhin, B. J.; Lee, S. J.; Kim, K. S. *Phys. Rev. A* **1993,** *48*, 3764; (e) Mhin, B. J.; Kim, J.; Lee, S.; Lee, J. Y.; Kim, K. S. *J. Chem. Phys.* **1994,** *100*, 4484; (f) Kim, J.; Mhin, B. J.; Lee, S. J.; Kim, K. S. *Chem. Phys. Lett.* **1994,** *219*, 243; (g) Kim, J.; Lee, J. Y.; Lee, S.; Mhin, B. J.; Kim, K. S. *J. Chem. Phys.* **1995,** *102*, 310; (h) Kim, J.; Kim, K. S. *J. Chem. Phys.* **1998**, *109*, 5886; (i) Kim, J.; Majumdar, D.; Lee, H. M.; Kim, K. S. *J. Chem. Phys.* **1999,** *110*, 9128.
20. (a) Steinbach, C.; Andersson, P.; Kazimirski, J. K.; Buck, U.; Buch, V.; Beu, T. A. *J. Phys. Chem. A* **2004,** *108*, 6165; (b) Lilach, Y.; Buch, V.; Asscher, M. *J. Chem. Phys.* **2003,** *119*, 11899; (c) Buch, V.; Devlin, J. P. *J. Chem. Phys.* **1999,** *110*, 3437; (d) Burnham, C. J.; Xantheas, S. S. *J. Chem. Phys.* **2002,** *116*, 1479; (e) Xantheas, S. S.; Miller, M. A.; Applegate, B. E.; Miller, R. E. *J. Chem. Phys.* **2002,** *117*, 1109; (f) Fajardo, M. E.; Tam, S. *J. Chem. Phys.* **2001,** *115*, 6807.
21. (a) Liu, K.; Brown, M. G.; Carter, C.; Saykally, R. J.; Gregory, J. K.; Clary, D. C. *Nature* **1996,** *381*, 501; (b) Huisken, F.; Kaloudis, M.; Kulcke, A. *J. Chem. Phys.* **1996,** *104*, 17; (c) Paul, J. B.; Collier, C. P.; Scherer, J. J.; O'Keefe, A.; Saykally, R. J. *J. Phys. Chem.* **1997,** *101*, 5211.
22. Steinbach, C.; Andersson, P.; Melzer, M.; Kazimirski, J. K.; Buck, U.; Buch, V. *Phys. Chem. Chem. Phys.* **2004,** *6*, 3320.
23. Miller, R. E.; Nauta, K. *Science* **1999,** *283*, 1895.
24. Howard, B. J.; Dyke, T. R.; Klemperer, W. *J. Chem. Phys.* **1984,** *81*, 5417.
25. Guedes, R. C.; Couto, P. C. D.; Cabral, B. J. *J. Chem. Phys.* **2003,** *118*, 1272.
26. Rincon, L.; Almeida, R.; Garcia-Aldea, D.; Riega, H. D. *J. Chem. Phys.* **2001,** *114*, 5552.
27. (a) Karpfen, A. J. *J. Phys. Chem.***1996,** *100*, 13474; (b) Karpfen, A. J. *J. Phys. Chem.* **1998,** *102*, 9286.
28. (a) Soper, A. K.; Bruni, F.; Ricci, M. A. *J. Chem. Phys.* **1997,** *106*, 247; (b) Lonsdale, K. *Proc. R. Soc. London, Ser. A* **1958,** *247*, 424; (c) Peterson, S. W.; Levy, H. A. *Acta Crystallogr.* **1957,** *10*, 70.
29. Suhai, S. *J. Chem. Phys.* **1994,** *101*, 9766; Suhai, S. *J. Phys. Chem.* **1995,** *99*, 1172.
30. (a) Hermansson, K.; Alfredsson, M. *J. Chem. Phys.* **1999,** *111*, 1993; (b) Ojamae, L.; Hermansson, K. *J. Phys. Chem.* **1994,** *98*, 4271.
31. Masella, M.; Flament, J. P. *J. Chem. Phys.* **1998,** *108*, 7141.
32. Etter, M. C.; Urbanczyk-Lipkowska, Z.; Jahn, D. A.; Frye, J. *J. Am. Chem. Soc.* **1986,** *108,* 5871.
33. (a) Dannenberg, J. J. *J. Mol. Struct.* **2002**, *615*, 219; (b) Simon, S.; Duran, M.; Dannenberg, J. J. *J. Phys. Chem. A* **1999,** *103*, 1640; (c) Masunov, A.; Dannenberg, J. J. *J. Phys. Chem. B* **2000**, *104*, 806; (d) Dannenberg, J. J.; Haskamp, L.; Masaunov, A. *J. Phys. Chem. A* **1999,** *103,* 7083.
34. Zhao, Y.-L.; Wu, Y.-D. *J. Am. Chem. Soc.* **2002**, *124*, 1570.
35. Suh, S. B.; Kim, J. C.; Choi, Y. C.; Yun, S.; Kim, K. S. *J. Am. Chem. Soc.* **2004,** *126*, 2186.
36. (a) Wang, Y.; Perdew, J. P. *Phys. Rev. B* **1991,** *43*, 8911; (b) Perdew, J. P.; Wang, Y. *Phys. Rev. B* **1992,** *45*, 13244.
37. Vanderbilt, D. *Phys. Rev. B* **1990,** *41*, 7892.
38. (a) Kim, K. S.; Oh, K. S.; Lee, J. Y. *Proc. Natl. Acad. Sci. U.S.A.* **2000,** *97*, 6373; (b) Oh, K. S.; Cha, S.-S.; Kim, D.-H.; cho, H.-S.; Ha, N.-C.; Choi, G.; Lee, J. Y.; Tarakeshwar, P.; Son, H. S.; Choi, K. Y.; Oh, B.-H.; Kim, K. S. *Biochemistry* **2000,** *39*, 13891; (c) Kim, K. S.; Kim, D.; Lee, J. Y.; Tarakeshwar, P.; Oh, K. S. *Biochemistry* **2002,** *41*, 5300; (d) Cho, H.-S.; Ha, N.-C.; Choi, G.; Kim, H.-J.; Lee, D.; Oh, K. S.; Kim, K. S.; Lee, W.; Choi, K. Y.; Oh, B.-H. *J. Biol. Chem.* **1999,** *274*, 32863; (e) Manojkumar, T. K.; Cui, C.; Kim, K. S. *J. Comput. Chem.* **2005,** *26*, 606.
39. (a) Cleland, W. W.; Kreevoy, M. M. *Science* **1994,** *264*, 1887; (b) Frey, P. A.; Whitt, S. A.; Tobin, J. B. *Science* **1994,** *264*, 1927.
40. (a) Wu, Z. R.; Ebrahimian, S.; Zawrotny, M. E.; Thornburg, L. D.; Perez-Alvarado, G. C.; Brothers, P.; Pollack, R. M.; Summers, M. F. *Science* **1997,** *276*, 415; (b) Warshell, A.; Parazyan, *Proc. Natl. Acad. Sci. U.S.A.* **1996,** *93*, 13665.
41. (a) Kim, S. W.; Cha, S.-S.; Cho, H.-S.; Kim, J.-S.; Ha, N.-C.; Cho, M.-J.; Joo, S.; Kim, K.-K.; Choi, K. Y.; Oh, B.-H. *Biochemistry* **1997,** *36*, 14030; (b) Cho, H.-S.; Choi, G.; Choi, K. Y.; Oh, B.-H. *Biochemistry* **1998,** *37*, 8325.
42. (a) Zhao, Q.; Abeygunawardana, C.; Talalay, P.; Mildvan, A. S. *Proc. Natl. Acad. Sci. U.S.A.* **1996,** *93*, 8220; (b) Li, Y. K.; Kuliopulos, A.; Mildvan, A. S.; Talalay, P. *Biochemistry* **1993,** *32*, 1816; (c) Petrounia, I. P.; Pollack, R. M. *Biochemistry* **1998,** *37*, 700.
43. Jeziorski, B.; Moszynski, R.; Ratkiewicz, A.; Rybak, S.; Szalewicz, K.; Williams, H. L. *Methods and Techniques in Computational Chemistry: METECC-94, Medium Size Systems*; Clementi, E., Ed.; STEF: Cagliari, 1993; Vol. B.
44. (a) Oh, K. S.; Lee, C.-W.; Choi, H. S.; Lee, S. J.; Kim, K. S. *Org. Lett.* **2000,** *2*, 2679; (b) Buhlmann, P.; Pretsch, E.; Bakker, E. *Chem. Rev.* **1998,** *98*, 1593.
45. (a) Mizuno, T.; Wei, W.-H.; Eller, L. R.; Sessler, J. L. *J. Am. Chem. Soc.* **2002,** *124*, 1134; (b) Yamaguchi, S.; Akiyama, S.; Tamao, K. *J. Am. Chem. Soc.* **2001,** *123*, 11372; (c) Anzenbacher, Jr., P.; Jursíková, K.; Lynch, V. M.; Gale, P. A.; Sessler, J. L. *J. Am. Chem. Soc.* **1999,** *121*, 11020; (d) McCleskey, S. C.; Griffin, M. J.;

Schneider, S. E.; McDevitt, J. T.; Anslyn, E. V. *J. Am. Chem. Soc*. **2003,** *125*, 1114; (e) Baldini, L.; Wilson, A. J.; Hong, J.; Hamilton, A. D. *J. Am. Chem. Soc*. **2004**, *126*, 5656; (f) Schmuck, C.; Geiger, L. *J. Am. Chem. Soc*. **2004,** *126*, 8898.

46. (a) Kim, S. K.; Singh, N. J.; Kim, S. J.; Kim, H. G.; Kim, J. K.; Lee, J. W.; Kim, K. S.; Yoon, J. *Org. Lett*. **2003**, *5*, 2083; (b) Yoon, J.; Kim, S. K.; Singh, N. J.; Lee, J. W.; Yang, Y. J.; Chellappan, K.; Kim, K. S. *J. Org. Chem*. **2004**, *69*, 581; (c) Chellappan, K.; Singh, N. J.; Hwang, I.-C.; Lee, J. W.; Kim, K. S. *Angew. Chem. Int. Ed*. **2005,** *44*, 2899; *Angew. Chem*. **2005**, *117*, 2959.
47. Streitwieser, A.; Heathcock, C. H.; Kosower, E. M. *Introduction to Organic Chemistry*; Macmillan: New York, 1992, 4th ed., p. 1101.
48. Lee, H. M.; Kim, J.; Lee, S.; Mhin, B. J.; Kim, K. S. *J. Chem. Phys*. **1999,** *111*, 3995.
49. (a) Kim, K. S.; Cui, C.; Cho, S. J. *J. Phys. Chem. B* **1998,** *102*, 461; (b) Suh, S. B.; Cui, C.; Son, H. S.; U, J. S.; Won, Y.; Kim, K. S. *J. Phys. Chem. B* **2002,** *106*, 2061.
50. (a) Kim, K. S.; Tarakeshwar, P.; Lee, H. M. In *Dekker Encyclopedia of Nanoscience and Nanotechnology*; Schwarz, J. A., Contescu, C., Putyera, K., Eds.; Marcel Dekker Inc.: New York, 2004; Vol. 3, pp. 2423–2433; (b) Kim, K. S. *Bull. Korean Chem. Soc*. **2003,** *24*, 757; (c) Tarakeshwar, P.; Kim, D.; Lee, H. M.; Suh, S. B.; Kim, K. S. In *Computational Material Science*; Leszczynski, J., Ed.; Elsevier: Amsterdam, 2004, pp. 119–170.